Biochimica et Biophysica Acta 1837 (2014) 578–588

Contents lists available at ScienceDirect

Biochimica et Biophysica Acta

journal homepage: www.elsevier.com/locate/bbabio

Review

Structure determination of α-helical membrane proteins by solution-state NMR: Emphasis on retinal proteins☆

Antoine Gautier *

Paul Scherrer Institute, Biomolecular Research Laboratory, OFLG/102, 5232 Villigen, Switzerland

ARTICLE INFO

Article history:
Received 10 May 2013
Accepted 24 June 2013
Available online 2 July 2013

Keywords:
Solution-state NMR
Membrane proteins
Protein structure determination
Expression systems
Isotope labeling

ABSTRACT

The biochemical processes of living cells involve a numerous series of reactions that work with exceptional specificity and efficiency. The tight control of this intricate reaction network stems from the architecture of the proteins that drive the chemical reactions and mediate protein–protein interactions. Indeed, the structure of these proteins will determine both their function and interaction partners. A detailed understanding of the proximity and orientation of pivotal functional groups can reveal the molecular mechanistic basis for the activity of a protein. Together with X-ray crystallography and electron microscopy, NMR spectroscopy plays an important role in solving three-dimensional structures of proteins at atomic resolution. In the challenging field of membrane proteins, retinal-binding proteins are often employed as model systems and prototypes to develop biophysical techniques for the study of structural and functional mechanistic aspects. The recent determination of two 3D structures of seven-helical trans-membrane retinal proteins by solution-state NMR spectroscopy highlights the potential of solution NMR techniques in contributing to our understanding of membrane proteins. This review summarizes the multiple strategies available for expression of isotopically labeled membrane proteins. Different environments for mimicking lipid bilayers will be presented, along with the most important NMR methods and labeling schemes used to generate high-quality NMR spectra. The article concludes with an overview of types of conformational restraints used for generation of high-resolution structures of membrane proteins. This article is part of a Special Issue entitled: Retinal Proteins — You can teach an old dog new tricks.

1. Introduction

Membrane proteins represent approximately 30% of proteins encoded by all genomes. They are involved in a numerous range of important cellular functions such as transport, cell-to-cell communication and signaling. Membrane proteins represent 50% of the sites of action for known drugs and are therefore highly desirable targets for the pharmaceutical industry [1]. However, membrane protein structures at atomic resolution constitute less than 1% of the 3D structures deposited in the Protein Data Bank (PDB) [2]. These structures have been predominantly solved by the use of X-ray crystallography and to a lesser extent by cryo-EM, solution and solid-state NMR. Despite this exciting progress, membrane protein structure determination remains a challenge, even for X-ray crystallography, which requires the growth of high-quality crystals from aqueous solutions of detergent-solubilized proteins [3]. For this reason, biomolecular NMR is a powerful complementary technique to X-ray crystallography and, beyond being applied to structure determinations, can also provide additional information about the internal mobility and dynamics of structural elements within the protein. Recent successes in structural studies of integral membrane proteins (IMPs) by solution NMR spectroscopy have been achieved in both the α-helical transmembrane class (49 superfamilies) and the β-barrel transmembrane class (17 superfamilies) [4,5]. This review aims to summarize some of the advances for the retinal proteins of the α-helical class, with particular focus on techniques for expression and labeling, the NMR methodology and the structure calculation process. Despite encouraging improvements that have been made over the last few years, no discussion of solid-state NMR studies will be included in the NMR spectroscopy methods and structure determination chapters. Instead, the reader is directed towards several reviews [6,7].

2. Production of isotopically labeled membrane protein samples

The limited structural information obtained on integral membrane proteins by the use of solution NMR can be attributed to several factors. Typically, only a low-yield expression of the desired isotopically labeled membrane protein can be achieved. In addition, poor stability, inadequate or insufficient isotope labeling and the size of the resulting protein–detergent complex, which can be too large to be

☆ This article is part of a Special Issue entitled: Retinal Proteins —You can teach an old dog new tricks.

* Tel.: +41 563105777; fax: +41 563105288.
E-mail address: antoine.gautier@psi.ch.

0005-2728/$ – see front matter © 2013 Published by Elsevier B.V.
http://dx.doi.org/10.1016/j.bbabio.2013.06.009

amenable to solution NMR techniques, represent several fundamental problems to be circumvented before structural analysis of the membrane protein can begin.

2.1. Overview of different expression systems

The over-expression of α-helical membrane proteins for biomolecular NMR requires the incorporation of magnetically active isotopes such as ^{13}C, ^{15}N and sometimes ^{19}F in order to exploit the full potential of multidimensional multinuclear NMR experiments [8,9]. Crucially, and more challenging from an expression perspective, samples are also required in which the majority of protons (^{1}H) are replaced by deuterons (^{2}H). Typically, high-quality NMR samples must contain near-millimolar concentrations of protein and be stable over prolonged periods of time.

The choice of expression system is usually dictated by the labeling scheme, which is itself determined by both the aim of the study and the type of NMR experiments to be undertaken. When the goal is to determine the 3D structure of an IMP and to study its backbone and/or side-chain dynamics, one must accomplish uniform isotopic labeling of the protein. Several research groups have shown that numerous membrane proteins can be cloned and expressed in large quantities in *E. coli* [10]. It has also been demonstrated that many integral membrane proteins can be expressed in minimal media, allowing isotopic labeling for screening of NMR sample conditions [11]. While the use of BL21(DE3) host cells has been successful for this purpose, several other host cell variants derived from BL21(DE3), such as Tuner, Rosetta (DE3), BL21(DE3)RP, BL21(DE3) RIL, and especially C41(DE3) and C43(DE3) have been proposed to reduce cytotoxic effects and often result in higher over-expression yields [12]. C41(DE3) and C43(DE3), for example, contain phenotypically selected genetic mutations that prevent the cell death associated with the expression of heterologous membrane proteins. Another derivative strain of BL21(DE3), Lemo21(DE3), is tunable for the over-expression of proteins and appears to be ideal for screening procedures of IMPs [13].

Two production strategies are available for the expression of membrane proteins in *E. coli* cells. The first involves the over-expression of the IMP into inclusion bodies, after which it is extracted with denaturing agents such as urea and guanidine hydrochloride. This is performed in the presence of harsh detergents such as SDS (sodium dodecyl sulfate) or SLS (sodium lauroyl sarcosinate), after which the denatured IMP is purified. The final stage is in vitro refolding and reconstitution of the denatured IMP into detergent micelles or another suitable membrane-mimetic medium [14]. For NMR studies, this strategy has been primarily applied to the more well-behaved β-barrel membrane proteins [15–18] but also to some α-helical IMPs [19–22]. This method can sometimes require the fusion of an N-terminal partner peptide with a high fraction of both charged residues and β-turn-forming residues to target the recombinant protein into inclusion bodies [23].

The second production strategy is to constitutively express and fold the protein of interest in the inner cell membrane, as demonstrated for the proteins DsbB [24], UCP2 [25] and NpSRII [26]. The protein is subsequently extracted from the membranes into mild detergents such as n-decyl-β-D-maltopyranoside (DM) or n-dodecyl-β-D-maltopyranoside (DDM) and purified in its native folded state. However, with most eukaryotic membrane proteins this strategy leads to severe cellular toxicity and low levels of expression. For this reason, the selection and modification of a signal peptide and/or the co-expression of proteins that assist the translocation and folding of the IMP are generally required [27,28]. Removal of the co-expressed protein and/or signal peptide during purification is made possible by adding an appropriate protease cleavage site during the cloning of the IMP into the expression vector.

Incorporation of ^{15}N and ^{13}C into the IMP involves the growth of *E. coli* cells in minimal media such as M9 or MOPS, thereby allowing controlled supplementation of nitrogen and carbon sources [29,30]. While the choice of the nitrogen source is generally ^{15}N-labeled ammonium chloride, there are several available carbon sources including acetate, glucose, glycerol, pyruvate and succinate [31]. The choice depends on the cost and the desired labeling scheme. Deuteration, where protons in the IMP are replaced with deuterons, reduces the overall proton density. This improves the relaxation properties of both the remaining protons and the heteronuclei ^{13}C and ^{15}N [32]. The ^{13}C and ^{15}N-labeling schemes do not interfere with the requirements for deuteration. However, if the protein is to be deuterated to a high level, then the carbon source must also be deuterated. This will significantly increase the costs of sample preparation. In order to achieve a high deuteration level (beyond 75%), *E. coli* cells must be grown in a D_2O-based medium that strictly excludes any H_2O. To achieve this, a process of gradual adaptation to acclimatize the cells to D_2O is used to palliate the toxic effects of D_2O on cell metabolism [33].

Uniform deuterium labeling increases the performance of amide-based backbone assignment schemes because it removes all the non-exchangeable protons in the IMP. However, the lack of protons on the side-chains leads to a dramatic reduction in the number of NOEs, meaning that there will generally be insufficient distance information for a high-resolution structure determination. This problem is more fundamentally limiting for helical membrane proteins, where the remaining inter-amide NOEs only define the secondary structure in the individual helices (for β-barrel IMPs, the network of cross-strand inter-amide NOEs also defines the tertiary backbone fold). To circumvent this issue, a limited subset of protons can be selectively reintroduced to the otherwise perdeuterated protein through the addition to the growth medium of specifically labeled amino-acids such as alanine [34], methionine [35] and aromatic residues [36], or biosynthetic amino-acid precursors such as α-ketobutyrate and α-ketoisovalerate [37,38].

In spite of the versatile isotopic labeling schemes and the numerous vectors and host strains available for the production of IMPs in *E. coli*, this expression system has some major drawbacks when compared to other available expression systems. *E. coli* cells are unable to perform the post-translational modifications of higher organisms and have slightly different codon usage. They also lack some eukaryotic membrane components, including cholesterol, and contain a substantial number of contaminating proteins that possess a high affinity for the divalent cations such as nickel, cobalt and copper that are exploited in the most widely used purification technique, immobilized metal affinity chromatography (IMAC) [39].

An alternative to this prokaryotic expression system is the unicellular eukaryotic yeast *Pichia pastoris* [40], which allows cheap uniform isotopic enrichment of IMPs [41,42], including perdeuteration [43–45]. Importantly, *P. pastoris* is able to perform the post-translational modifications found in higher eukaryotic membrane proteins [46]. Another advantage of *Pichia* over *E. coli* is that *Pichia* is capable of correctly forming the disulfide bonds generally found in eukaryotic IMPs [47]. However, the membrane composition of this expression system remains quite different to that in higher eukaryotes and may hamper the correct translocation and folding of some IMPs. It also has a relatively thick cell wall that may impede purification. Despite this, the Brown and Ladizhansky laboratories have doubly ($^{13}C/^{15}N$) isotopically labeled the fungal rhodopsin protein from *Leptosphaeria maculans* [48] and the human membrane protein aquaporin-1 [49] for solid-state NMR studies.

In order to produce recombinant protein in *Pichia*, the gene of interest is cloned into a suitable expression vector, after which the plasmid is linearized to stimulate recombination and transformed into protease-deficient *P. pastoris* strains such as KM71, MC100-3 SMD1163, SMD1165 or SMD1168H, where it will be integrated into the *Pichia*

genome. Initial growth in glycerol- or glucose-containing media is recommended in order to reach a critical biomass and induction is then achieved by addition of methanol. This induces the expression of the *alcohol oxidase 1* gene, which in turn drives the expression of the gene of interest. Uniform isotope labeling is achieved using a minimal medium for fermentative growth with undiluted and ^{15}N-labeled ammonium hydroxide as both a base and the sole nitrogen source. A modified and cheaper version of this scheme uses ^{15}N-labeled ammonium sulfate or ^{15}N-labeled ammonium chloride in combination with sodium hydroxide [50]. For growth in shake flasks, recent studies have used complex medium supplemented with ^{15}N-labeled ammonium sulfate and ^{13}C glucose before induction with ^{13}C methanol [51]. The possibility for selective labeling has been demonstrated by Whittaker and coworkers [52] but has very limited scope when compared to *E. coli*.

Cell-free (or in vitro) expression systems can also be used in the preparation of samples for biochemical and biophysical studies of IMPs [53,54]. The protein translational machinery of eukaryotic or prokaryotic cells is isolated, thereby allowing protein production to take place in an artificial environment. In addition to the cell-free extract, the basic reaction components required are the T7 RNA polymerase, which controls transcription, along with reducing agents to stabilize the enzyme and nucleoside triphosphates as substrates for translation. Amino-acids, PEG, Mg^{2+} and K^{+} are also critical for efficient expression [55]. Finally, a DNA-template with a standard T7 promoter and an efficient T7 terminator are necessary. In the special case of IMP expression, detergents, lipids or polymers [56,57] that do not interfere with the expression machinery can be added to the reaction mixture to immediately stabilize the protein in solution as it is translated. Otherwise, the protein of interest is expressed as a precipitate that can be solubilized by gentle agitation in mild detergents. This synthetic system allows the integration of amino-acids with the desired labeling pattern suitable for NMR studies [58]. The low level of metabolic activity reduces the scrambling of labeled isotopes, allowing near-total control over labeling strategies, which is essential for structural investigation of IMPs by NMR. In general, the highest rates of protein production are achieved by using continuous exchange or continuous flow set-ups in which the reaction mixture holding the high-molecular-weight compounds is separated by a semi-permeable dialysis membrane from the feeding mixture containing the low-molecular-weight precursors. Cell-free expression also offers the advantage of producing only the gene of interest with labeled isotopes, which in theory allows specific NMR observation of the expressed protein after only minimal purification procedures.

One of the most recent successes in which a cell-free expression system was used to produce an IMP for structure determination by solution NMR was achieved for the helical protein proteorhodopsin (PR) [59]. For the production of uniformly ^{15}N-labeled, ^{13}C,^{15}N-labeled and ^{2}H,^{13}C,^{15}N-labeled PR, commercially available amino-acid mixtures were simply added to the reaction mixture. By simultaneously adding a mixture of labeled and unlabeled amino-acids according to the desired labeling scheme, Reckel and co-workers produced an extensive range of selectively labeled samples. In addition, the use of stereo-array isotope labeling (SAIL) technology was used to reduce spectral broadening and overlap problems. This method relies on the use of stereo- and regio-specifically synthesized amino-acids to produce proteins with only one proton at every methylene carbon position, stereospecifically ^{13}C,^{1}H-labeled prochiral methyl groups and alternating ^{13}C,^{1}H/^{12}C,^{2}H labeling of aromatic moieties. Although this versatile method offers complete control of the labeling scheme, it is a relatively expensive technique. More recently the cell-free expression system was used in the Wagner laboratory to study different membrane-mimetic media by biophysical techniques and solution NMR [60]. In this study nine double- or triple-labeled samples of bacteriorhodopsin (bR) were made by using two commercially available algal amino-acid mixtures supplied with unlabeled amino-acids to generate different isotope-labeled samples. The level of deuteration was estimated to be above 90%.

For the study of higher eukaryotic membrane proteins by NMR in which expression of the functional IMP is not possible in the *E. coli*, *Pichia* or cell-free expression systems, a few other eukaryotic expression hosts are available. Unfortunately, these systems generally have only low-to-moderate yields, are expensive and, most crucially, have a very limited scope for isotope-labeling schemes. In cases where uniform labeling is not necessary, for example where the aim is not to solve the 3D structure but to map the diverse interactions of an IMP (as for rhodopsin [61,62]) or to detect motions and conformational changes within the protein [63], some sparse labeling schemes involving either single amino acids or single amino acid types are possible. The baculovirus–insect cell expression system has been successfully used for amino acid-specific labeling [64,65] and uniform labeling [66,67] of soluble proteins. The basis of the technique involves two steps. First, the gene of interest is cloned into a plasmid transfer vector downstream of the polyhedrin baculoviral promoter. Then the plasmid is introduced, along with genomic viral DNA, into insect cells such as *Spodoptera frugiperda* or *Trichoplusia ni*. The heterologous gene is expressed, usually during the late stages of infection. The protein is subsequently processed and targeted to its final cellular location.

The strategies for isotopic labeling in the baculovirus system are very simple. The amino acid of interest can be replaced by its labeled version in the insect cell medium when the medium is made from scratch [68]. The low level of metabolic activity present in this system reduces the scrambling of labeled isotopes through undesired metabolic pathways. In addition, custom-made synthetic drop-out medium derived from commercially available protein-free medium can be used, as demonstrated for visual rhodopsin [69,70]. In this work, [αε-$^{15}N_2$]-labeled lysine and aromatic ring-$^{2}H_4$-labeled tyrosine rhodopsin was expressed by substituting the relevant unlabeled amino acids by their corresponding labeled versions, leading to the first NMR spectra of an IMP produced with the baculovirus–insect cell expression system.

Another approach using cell lines from higher eukaryotic hosts, which is contributing to both the general field of retinal proteins and NMR of membrane proteins, is the use of mammalian cells. However, uniform isotope labeling in mammalian cells such as CHO, HEK, BHK21, HT1080 or Namalwa is rather expensive and frequently yields only small quantities of protein. The heterologous expression of an IMP was first established for unlabeled rhodopsin, where the wild-type opsin gene was co-transfected with another plasmid conferring tetracycline resistance into HEK293S cell lines. The cells expressing the selectable marker were screened for drug resistance to identify a stable cell line that expressed opsin [71]. Researchers have subsequently focused their efforts on amino-acid specific labeling in mammalian cells. Different laboratories have successfully managed to incorporate ^{15}N-labeled lysine, ^{13}C-labeled glycine [72,73], α,ε-^{15}N-labeled tryptophan [74] and also a mixture of amino acids (^{15}N/^{13}C GKLQSTV(W)) [75] into wild-type and mutant H65C/C140S rhodopsin. The labeled amino acids were simply added to cell culture medium lacking the appropriate amino acids.

2.2. Membrane-mimetic media for NMR studies of IMPs

Solution NMR spectroscopy of membrane proteins generally relies on their solubilization in a micelle-forming detergent. The objective is to obtain a mono-disperse protein–detergent complex in which the protein adopts its native fold while keeping the molecular weight of the complex as low as possible. The detergent monomers that encapsulate the hydrophobic regions of the IMP confer solubility in aqueous solutions but dramatically increase the overall molecular weight. As a consequence, the tumbling (or rotational diffusion) rate becomes slower, which consequently increases the transverse relaxation rates of the nuclear spin states. The faster transverse relaxation not only leads to greater intensity losses during magnetization transfer

steps, but also broadens the resonance linewidths, with both effects resulting in reduced signal-to-noise ratios. The line-broadening also leads to increased peak overlap, greatly complicating spectral interpretation. In terms of size, membrane proteins bound to detergent behave as much larger proteins (ca. 75–100 kDa), but with comparatively fewer resonances.

The introduction of new approaches such as specific isotopic labeling schemes [76], novel spectroscopic techniques [77] and more sensitive equipment [78] have allowed the molecular-weight limit of solution NMR to be pushed ever higher, with systems in excess of 100 kDa now amenable to structural characterization by solution NMR. Nevertheless, for membrane proteins it is clear that the detergent introduces more difficulties than merely an increase in the effective size of the protein. If too few detergent molecules are available to satisfy the hydrophobic surface of each protein molecule, then oligomerization will occur, resulting in the formation of even larger complexes. However, if the concentration of detergent is too high, then the viscosity of the solution is significantly increased, further reducing the tumbling rate of the protein–detergent complex and ultimately leading to uninterpretable spectra [79].

Given the large number of detergents available, choosing an appropriate detergent can be a lengthy process [80]. Some of the general properties of detergents can be used to guide the selection of suitable candidates for screening. The critical micellar concentration (CMC) is the concentration above which additional monomers assemble to form micelles. The CMC decreases with the length of the alkyl chain and increases with the introduction of double bonds and branch points. The aggregation number is the number of detergent molecules contained in a single micelle. The hydrophilic–lipophilic balance (HLB) indicates how hydrophilic a detergent is, with large values corresponding to more hydrophilic detergents. Detergents with a HLB of 12 to 20 are preferred for non-denaturing solubilization of membrane proteins. The performance of a detergent also depends on its concentration, alkyl chain length and purity, and also on the presence of organic additives, temperature and pH and ionic strength of the buffer.

Detergents that have been used successfully for solution-state NMR spectroscopy of both classes of IMPs include N,N-dimethyldodecylamine N-oxide (LDAO), sodium dodecyl sulfate (SDS), CYFOS-7, n-octyl-β-D-glucoside (β-OG) and n-dodecylphosphocholine (DPC) [81]. Some of these detergents are also available in a deuterated form. However, it appears that, from a relaxation perspective, there is no significant benefit in using perdeuterated detergents for the final stage of NMR sample preparation as no improvement in the quality of the NMR spectra has been observed [82]. This indicates that detergent–protein interactions are not a major source of spin relaxation. In terms of side-chain assignment, however, the use of deuterated detergents will invariably improve the quality of the NMR spectra by largely removing t_1-noise stripes associated with imperfect suppression of strong protonated detergent signals. In addition, genuine peaks arising from detergent protons attached to ^{13}C at natural abundance, which can be at least as intense as protein signals, are also removed [83].

The majority of high-resolution structures of IMPs solved by X-ray crystallography and NMR spectroscopy have resulted from the solubilization of the membrane proteins in a micellar environment. However, detergent micelles cannot fully mimic a lipid bilayer membrane due to their inherently dissimilar super-structure and their tendency to destabilize or change the biochemical properties of the IMP that they surround. This can be explained by their differences to natural lipids with respect to the charges of the head groups, the disparity in the length and number of the alkyl chains and also to the variation in lateral pressure applied to the membrane protein. Alternatives to traditional detergents can be found in the short-chain saturated phospholipids c6-DHPC and c7-DHPC, and also lysophospholipids such as LMPG, LMPC, LOPG and LPPG. The use of some of these phospholipids has led to the structure determination of several IMPs of different classes and sizes by solution NMR spectroscopy [16,26,59,84,85].

New perspectives on native bilayer substitution are also being provided by the application of nanodiscs [86]. These lipoproteins consist of two molecules of an amphipathic protein called membrane scaffold protein, which embeds lipids such as DMPC, POPC, POPS, POPE and POPG. Recent studies have demonstrated that IMPs reconstituted in nanodiscs can be studied by high-resolution solution NMR [87,88]. In parallel, other biophysical and structural studies employing non-traditional detergents indicate that these may be worthy of further investigation and screening for NMR studies. These compounds include steroid-based detergents [89], facial amphiphiles [90], fluorinated detergents [91], amphipols [92], neopentyl glycols [93] and peptide surfactants [94]. Extensive description and analysis of these novel-solubilizing agents can be found in multiple comprehensive reviews [95,96].

During the final stage of NMR sample preparation, one needs to consider not only the choice of detergent but also the absolute detergent concentration and, most importantly, the protein-to-detergent ratio. For example, two seven-transmembrane proteins (7-TM) gave different optimal detergent concentrations, with a 120-fold c7-DHPC excess found to be best for NpSRII, while an ~85-fold excess was optimal in the structural determination of PR (Table 1). DPC was used at a 112-fold excess for the protein DAGK [21] but only at a 7-fold excess for the tetrameric KcsA [97]. In addition — as for soluble proteins — searching for the appropriate temperature, pH, buffer system and ionic strength is critical for successful optimization of the sample conditions.

3. Solution NMR spectroscopy methods

3.1. Backbone resonance assignments

For the structure determination of IMPs by solution NMR spectroscopy, 1D and 2D NMR spectra have restricted application for resonance assignment, as the resonance overlap is severe. Spectral crowding can be reduced by the use of multidimensional multinuclear NMR experiments in combination with uniform ^{13}C,^{15}N labeling [8]. Typically, triple-resonance experiments are applied for the assignment of backbone moieties. These rely on the transfer of magnetization through large scalar couplings to connect the different heteronuclei in the protein backbone. In the case of NpSRII, pairs of out-and-back triple-resonance experiments were used to establish the sequential connectivity of the residues via matching of the

Table 1
Details of the structures of detergent-solubilized α-helical membrane proteins sensory rhodopsin II and proteorhodopsin.

	Sensory rhodopsin II	Proteorhodopsin
Organism	*Natronomonas pharaonis*	γ-*Proteobacterium*
Molecular weight (kDa)	26.4	26.0
Expression system	*E. coli*	Cell-free
NMR conditions		
Protein concentration	0.5 mM	0.3–0.5 mM
Detergent used	C7-DHPC	C7-DHPC
Detergent concentration	60 mM	42 mM
Temperature	323 K	323 K
Buffer system	50 mM sodium phosphate	25 mM sodium acetate
pH	6	5
Size of complex (kDa)	~70	~85
Conformational restraints		
H-bond	132	133
Dihedral angle	190	196
NOE	5564	239
RDC	–	81
PRE	–	1006
Other	–	4
Calculation program	CNS 1.1 and ARIA 1.2	CYANA
PDB entry (year)	2KSY (2010)	2L6X (2011)
Reference	[26]	[59]

chemical shifts of the $^{13}C\alpha$, $^{13}C\beta$ and ^{13}CO nuclei. The six pair-wise experiments required — HNCA/HN(CO)CA, HNCACB/HN(CO)CACB and HN(CA)CO/HNCO — are recorded on $^{2}H,^{13}C,^{15}N$-labeled protein samples [98]. For PR, the backbone assignment was obtained by recording TROSY-type BEST (bandwidth-selective excitation short-transient) versions of HNCA, HN(CO)CA, HNCACB and HNCO spectra in combination with 3D and 4D ^{15}N-separated NOESY spectra.

The high molecular weight of IMPs surrounded by detergents leads to slow molecular tumbling in aqueous solutions, and therefore fast transverse relaxation, which results in broad and weak lines, and severe loss of magnetization during transfer steps within the pulse sequences. As mentioned above, the relaxation properties of the backbone nuclei can be greatly improved by substitution of protons by deuterons. The magnetic moment of deuterons is approximately one-sixth that of protons, so that perdeuteration of the amino-acid side-chains dramatically reduces the total dipolar contribution to the transverse relaxation rates of the remaining protons and also the heteronuclei ^{13}C and ^{15}N. It is also worthwhile to mention that it is crucial to back-exchange all the amide deuterons for protons. After purification in H_2O-based buffers, back-exchange is often nearly complete. However, it can sometimes be difficult to exchange all the amide protons, particularly those buried in the core of the protein, such that development of unfolding/refolding protocols may be required [21].

In addition to perdeuteration, the use of transverse relaxation-optimized spectroscopy (TROSY) at high magnetic fields can further improve the relaxation properties of the backbone amide spin-system, allowing application of H^N-detected experiments, including triple-resonance assignment experiments, to ever-larger systems [99–101]. Cross-correlation between the ^{1}H or ^{15}N chemical shift anisotropy (CSA) and ^{1}H–^{15}N dipole–dipole relaxation mechanisms leads to differential relaxation of the individual components of the ^{1}H and ^{15}N doublets, respectively. The two components of each doublet have different linewidths due to either cancelation or reinforcement of the local fields due to the CSA and the magnetic dipole of the attached spin. TROSY is a form of line-selective spectroscopy that detects only the slow-relaxing doublet components in both ^{15}N and ^{1}H dimensions, while suppressing the other lines that have less favorable relaxation properties [102,103]. The size of the TROSY effect depends on the cross-correlation rate, which is approximately directly proportional to the rotational correlation time, and the strength of the magnetic field through its effect on the size of absolute magnitude of the CSAs. Hence, the relative benefit of ^{15}N-TROSY over traditional ^{15}N-HSQC-based techniques becomes more pronounced as the size of the protein increases and for a given system is maximized at fields of ~900 MHz and above (the optimum fields for the ^{1}H and ^{15}N TROSY effects are different due to their different CSAs). In addition, the maximum TROSY effect can only be realized if other relaxation pathways are suppressed, particularly those due to dipolar interactions with remote protons. Therefore, TROSY-based spectra are typically recorded on perdeuterated samples.

Another important contributor to the success of the backbone assignment is the use of non-uniform sampling (NUS) schemes [104] in combination with maximum entropy reconstruction [105] or other non-linear processing schemes. These can be employed in all indirect chemical shift evolution periods, maximizing the sensitivity per unit time, although the indirect ^{15}N dimension of the triple-resonance assignments is typically acquired in a constant-time fashion, so that sensitivity benefits are only expected from NUS in the indirect ^{13}C dimension. An alternative reconstruction technique for non-uniformly sampled data is the “compressed sensing” protocol recently developed by Nietlispach and co-workers, which leads to a large reduction in experiment time for non-sensitivity-limited experiments or sensitivity benefits without compromising spectral resolution [106,107]. Provided that peak overlap is not too severe, 3D ^{15}N-separated NOESY spectra on perdeuterated protein can be used to complement and/or confirm the backbone assignments. Indeed, short-range NOE cross-peaks between H^N_i to $H^N_{i \pm k}$ are normally intense, particularly in the characteristic α-helical secondary structures found in IMPs, and can be used for early identification of the transmembrane helices.

3.2. ^{1}H and ^{13}C side-chain resonance assignments

Typically, the strategy employed for the structure determination of IMPs, as with soluble proteins, is to first sequentially assign the backbone resonances and then to progress to the assignment of the side-chain resonances. Finally, assignment of NOESY spectra will allow the conversion of the measured NOEs into distance restraints for structure calculation. The backbone assignment of IMPs is achieved by recording multinuclear multidimensional NMR spectra on perdeuterated $^{13}C,^{15}N$-labeled samples. As mentioned earlier, back-exchange at labile proton sites leads to re-protonation of amides and amines, but the side-chains remain almost completely deuterated, and therefore only a relatively small number of NOEs, and hence distance restraints, can be measured. The reintroduction of a small number of additional protons via the selective methyl protonation of the hydrophobic amino acids (Ala β, Ile δ1, Leu δ, Met ε and Val γ) has become a common practice and is often applied to large proteins or complexes [108]. This robust and relatively cost-effective labeling scheme relies on the addition of biosynthetic precursors during cell growth of the prokaryotic expression system *E. coli*. Addition of α-ketobutyrate and α-ketoisovalerate to otherwise deuterated growth medium (using both D_2O and deuterated glucose) leads to selective protonation of the Ile δ1, Leu δ and Val γ methyl groups [38]. For the studies of the integrin αIIbβ3, NpSRII, DsbB or VDAC-1, U-[$^{2}H,^{13}C,^{15}N$], [$^{13}CH_3$]-Ile(δ1) [$^{13}CH_3/^{12}CD_3$]-Leu,Val-labeled (ILV) samples were produced (Fig. 1) and used for side-chain methyl resonance assignment. First, correlation of the methyl moieties with their corresponding backbone amides was achieved via COSY-type 3D Ile-(HM)CM(CGCBCA)NH, 3D Leu-(HM)CM(CGCBCA)NH and 3D Val-(HM)CM(CBCA)NH experiments. Then, the same methyl groups were correlated with their corresponding $^{13}C\alpha$ and $^{13}C\beta$ resonances using out-and-back-style 3D HMCM[CG]CBCA experiments. For the study of NpSRII, the high concentration of detergent created intense resonances and t_1-noise strips that overlapped with many of the ^{13}C protein resonances. The use of coherence-order-selection with pulsed field gradients was found to be beneficial in all methyl-detected NMR experiments by reducing the t_1-noise arising from the detergent signals. For NpSRII, in addition to this strategy, a fully protonated $^{13}C,^{15}N$-labeled sample was prepared and used to assign the majority of Ala, Ile γ2, Met and Thr methyl groups via a combination of CT-^{13}C-HSQC and 3D HCCH-COSY experiments. Using the same protonated sample, additional assignments of methylene and methanetriyl groups were obtained by analyzing 3D (H)CCH-COSY and 3D H(C)CH-COSY experiments in combination with 3D NOESY-^{13}C-HMQC and 3D NOESY-^{15}N-HSQC spectra. In 3D NOESY-^{13}C-HMQC spectra recorded on protonated and ILV-labeled samples, many short-range intra-residue and long-range inter-residue NOEs were observable and assignable. However, there was significant signal overlap in the methyl region and a large number of cross-peaks could not be assigned due to their proximity to the strong diagonal peaks. This overlap problem was exacerbated by the additional presence of NOE cross-peaks between the detergent and the protein. To overcome this problem a 4D HCCH-NOESY spectrum was recorded on ILV-labeled NpSRII but due to limited resolution and low signal-to-noise ratios, only 30 long-range inter-residue NOEs could be assigned in this spectrum.

For the study of PR, produced with the cell-free expression system, the sequence-specific assignment also started with the methyl-containing amino-acids. The methylene and methanetriyl groups of Ala, Ile, Leu, Met and Thr were first assigned using 3D (H)CCH-TOCSY experiments and then linked to methyl groups with HMCMCB or HMCMCBCA experiments. Combining the 3D COSY-type out-and-back experiments described above for NpSRII with 3D ^{13}C-separated NOESY

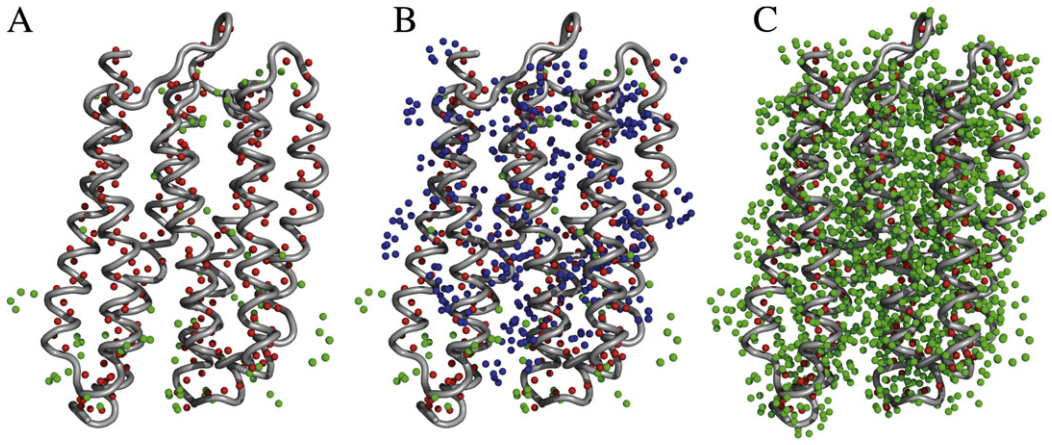

Fig. 1. Comparison of proton-labeling schemes achieved for sensory rhodopsin II NpSRII. A: The remaining protons of a $^{2}H,^{13}C,^{15}N$-labeled protein are the backbone amides protons (red) and the side-chain protons of Asn δ, Gln ε, Lys ζ, Arg $\eta^{1,2}$, Ser γ, Thr γ^{1} and Tyr η (green). B: The U-[$^{2}H,^{13}C,^{15}N$], [$^{13}CH_3$]-Ile(δ^{1}) [$^{13}CH_3/^{12}CD_3$]-Leu,Val-labeled NpSRII has the same labeling scheme as in A except that methyls of Ile δ, Leu δ and Val γ are also protonated (blue). C: Expression of ^{15}N- and $^{13}C,^{15}N$-labeled protein leads to perprotonation of NpSRII with more than 1900 protons.

and 4D $^{13}C,^{15}N$-separated NOESY spectra yielded the methyl side-chain assignments of oro-SAIL Leu- and Val-labeled samples. There are 10 Trp present in PR that are mostly localized in the hydrophobic transmembrane region, and hence their side-chain assignment was attempted by first linking the δ1-CH groups with the Cβ nuclei using ^{13}C-TROSY-HCD(CG)CB experiments. Then the indole group was assigned by recording a 3D ^{15}N-TROSY-HNC spectrum and finally the remaining four CH groups were assigned from a 3D NOESY-^{13}C-HMQC spectrum. The large number of contacts to Trp side-chain protons was extremely valuable for extracting both short-range, intra-residue and long-range distance restraints. However, in order to improve the quality of the structure, two more samples were prepared (ALVW- and AILMTVW-labeled PR), from which a substantial number of inter-methyl NOEs were identified by recording 4D SOFAST-methyl-TROSY HCCH-NOESY experiments.

4. Distance restraints for structure determination

3D structure calculations of soluble proteins and IMPs require all possible structural information on the protein of interest. A prerequisite for calculation of the 3D structure is the primary amino acid sequence. In most cases, a randomized extended conformation is created from the sequence as the initial structure from which the calculation proceeds, but the increasing sophistication of homology modeling programs and the emergence of software to predict 3D structures from NMR data allows folded models to be used as starting points for the structure calculation [109,110].

4.1. Hydrogen bonds and backbone dihedral angles

The backbone torsion angles of proteins can be predicted following the assignment of the backbone resonances. The backbone chemical shifts are used by dihedral prediction software to forecast the ϕ and ψ torsion angles. These programs, such as TALOS [111], TALOS+ [112] or DANGLE [113], use Hα, Cα, Cβ, C′ and N^{H} chemical shifts for a run of three or five consecutive residues to make a prediction for the dihedral angles of the central residue. These predictions can therefore be used to obtain secondary structure information, which can be confirmed with other related methods such as the classical chemical shift index (CSI) [114] or the secondary chemical shift difference $\Delta\delta_{C\alpha} - \Delta\delta_{C\beta}$. This analysis can be further extended by building hydrogen bond (H-bond) tables for amide protons. Experimentally, CLEANEX experiments [115] are used to infer which amide protons are involved in secondary structure H-bond networks by measuring the rate of solvent exchange. In addition, information from short-range inter-residue NOEs (H^{N}_{i} to $H^{N}_{i \pm k}$ with $k = 1, 2, 3$) identified during the backbone sequential assignment [59,98] can be incorporated to build reasonably well-defined individual helices. However, the overall tertiary structure will be ill-defined at this stage as no inter-helix distances are available to restrain the global fold. Therefore, other sources of distance restraints are required to orient the helices relative to each other, give them correct curvature and position the side-chains.

4.2. NOE-based restraints

As mentioned above, a high level of cross-peak assignment in the NOESY spectra is necessary to determine a high-resolution protein structure. Dipolar interactions between protons that are close in space give rise to cross-peaks in NOESY spectra. Typically, 3D ^{13}C-separated and ^{15}N-separated NOESY experiments that are recorded on protonated samples contain a very large number of NOE peaks. Substantial peak overlap together with limited spectral resolution may prevent a complete assignment of the inter-side-chain NOESY cross-peaks that represent an important source of long-range distance information.

On a typical protonated protein sample, only pairs of protons that are closer than about 6 Å give rise to detectable cross-peaks in NOESY spectra. NOE peaks that are observed and assigned then need to be converted into distance restraints. The peak heights of cross-peaks in NOESY spectra are typically used as proxies for the NOE peak volumes [116]. However, in a crowded NOESY spectrum it is often the case that each resolvable peak has contributions from multiple proton pairs. In addition, it can be difficult to identify all the contributions to a particular cross-peak, such that the peak cannot be assigned in one dimension. In this latter case, candidate protons for the unassigned dimension can be identified from the proton chemical shift list. In both cases, the peak height can be converted into an ambiguous distance restraint, a concept introduced by the program ARIA (Ambiguous Restraints for Iterative Assignment). ARIA (which is interfaced to the software CNS [117]) calculates structures in an iterative fashion, reducing the ambiguity of the distance restraints at each cycle by using the current trial structure to identify protons that cannot contribute to the ambiguous NOEs and discarding them from the candidate list for the ambiguous assignment. In addition, the calibration for the conversion of NOE peak intensities into distances is improved iteratively as the structure converges over the course of the calculation [118,119]. Eventually, ARIA filters and reduces the number of ambiguous assignment possibilities in order to obtain predominantly

unambiguous restraints in the last iteration. Other programs such as CYANA [120] and XPLOR-NIH [121] can also be used for automated NOE assignment and/or structure calculation and refinement. Overall, the methodology of these calculation programs is based on simulated-annealing molecular dynamics simulations with additional potential energy terms corresponding to the available NMR restraints [122].

4.3. Residual dipolar couplings

While the reduced number of protons in deuterated samples is important for backbone assignment, the corollary is that the number of detectable NOEs is drastically reduced, so that these are generally insufficient for a high-resolution structure determination. Selective re-protonation can lead to highly useful additional NOEs, but the distance-restraint density still remains significantly lower than would be achievable for typical small-to-medium-sized soluble proteins. However, the peak overlap in the NOESY spectra of fully protonated IMPs or large proteins is such that only partial assignment of the observable NOE cross-peaks is likely to be feasible. Thus additional structural restraints are required to improve the accuracy and precision of the NOE-based structures. Residual dipolar couplings (RDCs) can be exploited for characterization of protein dynamics and can provide angular restraints for structure refinement of soluble proteins and IMPs [123]. Typically, $^1D(\mathrm{N}–\mathrm{H}^{\mathrm{N}})$, $^1D(\mathrm{H}^{\alpha}–\mathrm{C}^{\alpha})$, $^1D(\mathrm{N}–\mathrm{C}')$, $^1D(\mathrm{C}'–\mathrm{C}^{\alpha})$ and $^2D(\mathrm{H}^{\mathrm{N}}–\mathrm{C}')$ couplings can be recorded on protein samples with ARTSY, IPAP-HSQC and TROSY-based HNCO-type experiments [124,125]. The measured dipolar coupling is determined by the ensemble-averaged orientation of the internuclear vector connecting the two coupled spins with respect to the magnetic field, and can be converted into orientational restraints within a molecular alignment frame. These distance-independent restraints can be beneficial for accurately orienting the different α-helical secondary structure elements of IMPs, as demonstrated by solution NMR studies of phospholamban [20], PR [59], DAGK [21], DsbB [24], UCP2 [25] and M2 [19]. There are numerous media available to generate partial alignment of the protein [126] but only relatively few are compatible with the presence of detergents or lipids. The use of stretched and compressed polyacrylamide gels has been successfully applied in recent years to provide the weak protein alignment required [127,128]. As for the choice of detergents to sustain IMPs in their native state, the exact conditions used to formulate these gels can have a strong effect of the resulting spectra, but to a large extent suitable formulations must be identified by a process of trial-and-error. From a steric perspective, different molar ratios of acrylamide and bis-acrylamide as well as different overall percentages of the gel can be tested. Some types of gel also have an electrostatic component [129,130] and these can be made positively or negatively charged by substituting the acrylamide with APTMAC or AMPS, respectively. Different net charges should lead to different anisotropic orientational probability distributions and hence provide additional sets of restraints. This is an important requirement since the angular restraints derived from RDCs are subject to a certain degree of degeneracy that can be reduced by measuring the same RDCs in different alignment media. More practically, the gels can be compressed laterally by casting them with diameters greater than the inner diameter of a NMR tube used. The transfer of the gel into the NMR tube can be achieved with a commercially available system [131] or by first drying the gel, transferring it to the tube in its dehydrated state and then rehydrating the gel with the protein–detergent solution. Longitudinally compressed gels can be produced by initially casting the gel in the NMR tube. The gel is then extruded, cut to a precise length, dried and finally rehydrated in the same NMR tube but with a plunger to restrain its longitudinal extension and hence create the anisotropic environment. The height of the plunger will dictate the degree of compression and therefore the size of the dipolar couplings recorded [24]. More recently, the structure determination of the membrane protein UCP2 highlighted the potential of a new medium, DNA-nanotubes, to induce alignment of IMPs [25].

4.4. Paramagnetic relaxation enhancements

In cases where structural restraints from long-range NOEs and/or RDCs are insufficient to accurately define the 3D structure, additional long-range distance restraints can be derived from the measurement of paramagnetic relaxation enhancements (PREs). This strategy relies on the attachment of a paramagnetic probe or spin-label, such as a nitroxide radical that possesses an unpaired but stable electron. For example the compound MTSL, which is derived from methanethiosulfonate, can be covalently attached to the target protein through formation of a disulfide bond to a free thiol group of an exposed cysteine residue [132]. The unpaired electron on the nitroxide group in this tag generates a strong dipolar magnetic field that strongly affects the spin relaxation properties of magnetic nuclei in the vicinity of the spin-label. These effects are called paramagnetic relaxation enhancements, the magnitudes of which are strongly dependent on the distance between the nuclear spin and the paramagnetic probe. There are several ways to measure paramagnetic relaxation enhancements. The most straightforward method, as used for PR, UCP2, ArcB, QscE, KdpD [84] and the presenilin-1 CTF [133], is to compare the signal intensities between HSQC or TROSY spectra of the MTSL-labeled protein with the attached radical either unquenched or quenched. The quenching can be achieved simply by addition of ascorbic acid to the sample. The relative attenuation of the signal intensities in the spectrum of the MTSL-labeled protein can be converted into distances between the nuclear spins and the spin label, providing additional distance restraints for structure calculation. This strategy has been effectively applied to the structure determinations of a dozen α-helical membrane proteins. A more rigorous approach is to record a set of amide proton T_2 relaxation experiments in the presence of the unquenched and quenched radical to directly derive the paramagnetic relaxation enhancement as the difference between the measured relaxation rates. PREs can also be measured using other paramagnetic probes such as metal-binding peptides or synthetic metal-chelating tags, which can then be used for refinement of IMP structures [134]. In addition to paramagnetic relaxation enhancements, both residual dipolar couplings and pseudo-contact shifts can be detected if the unpaired electron has an anisotropic g-tensor and these effects can be exploited for both structure determination and to extract additional information on dynamics and protein–ligand interactions. A more comprehensive description of the various tags, paramagnetic effects and their applications can be found in detailed reviews [135,136].

4.5. Structures of NpSRII and PR

The first solution NMR structures of seven-transmembrane α-helical proteins are both retinal proteins (Fig. 2). Except for the fact that these two IMPs were embedded in the same detergent and that the NMR experiments were recorded at the same temperature, it is remarkable to see that the strategies adopted are quite distinct (Table 1). The use of different expression systems yielded disparate labeling schemes and therefore different assignment methods for the backbone and side-chain resonances [59,98]. 96% and 100% of the backbone assignments were achieved for PR and NpSRII, respectively, while 44% of the side-chains in the PR trans-membrane region were assigned compared to 66% for NpSRII. The structure of the latter was solved with ARIA/CNS using NOE distance restraints alone [26]. The lower proportion of side-chain assignment for PR correspondingly reduced the number of assignable NOEs and hence long-range distance information. Compensating additional inter-helix restraints were derived from biochemical experiments, PREs and RDCs, which were combined with the available NOE restraints for structure calculation using CYANA. Structural validation of the two proteins in their micellar environments also differed significantly. For PR, titration experiments involving paramagnetic agents were used to discriminate solvent-accessible residues from the micelle-embedded amino acids of the transmembrane helices, while for NpSRII Ramachandran

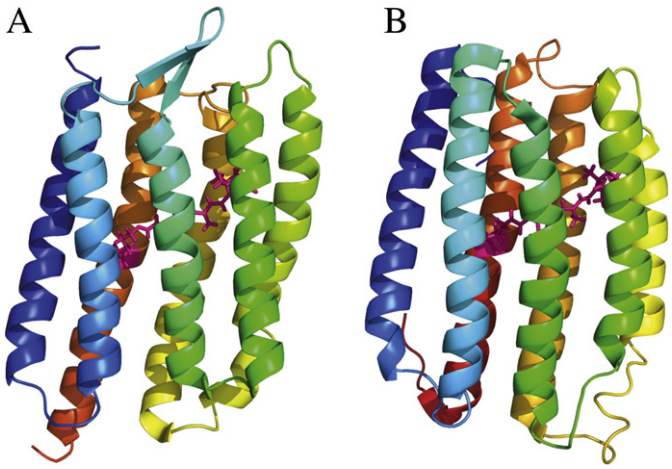

Fig. 2. Retinal membrane proteins determined by solution-state NMR spectroscopy. Cartoon representation viewed across the membrane using rainbow colors with blue for N-terminus and red for C-terminus of A: sensory rhodopsin II NpSRII [26] (PDB 2KSY) and B: proteorhodopsin PR [59] (PDB 2L6X). All-*trans* retinal is shown with sticks in pink.

analyses of the structure closest to the mean (Fig. 3) and the ensemble were performed using the programs PROCHECK [137] and PROCHECK-NMR [138], respectively. The structure of NpSRII was also found to be consistent with the two available crystal structures [139,140] while no crystal structures of PR have yet been made public. The most significant difference between the two retinal-binding structures is the absence of an anti-parallel β-sheet between helices II and III in PR, which instead appears to form a β-turn. The lengths of the helices in PR and NpSRII are similar and the same kink in helix V is observed in both structures. Slight bends are observed for helices IV and V of PR whereas all the helices in NpSRII tend to be straight. Except for the extra-cellular loop 2 (ECL2), which does not form a β-sheet in PR, the other intra- and extra-cellular loops are comparable in length. The two retinal-binding pockets have matching protein conformation with

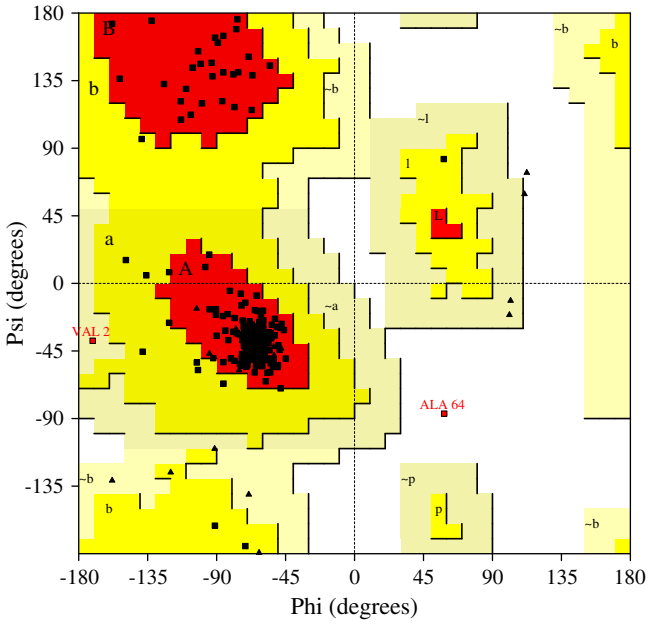

Fig. 3. Ramachandran plot generated by PROCHECK for the NpSRII structure that is the closest to the mean. 93.2% of the residues are classified as favored (red), 5.8% as allowed (yellow), 0.5% as generously allowed (cream) and 0.5% as disallowed (white). The sterically allowed regions correspond to β-sheet (labeled B, b and ~b), right-handed α-helix (A, a and ~a) and left-handed α-helix (L, l and ~l).

both Asp75 and Asp201 in NpSRII and the corresponding Asp97 and Asp227 residues in PR acting as counter-ions by pointing towards the protonated Schiff base.

5. Conclusion and perspectives

The view that solution-state NMR spectroscopy can play a pivotal role for structure determination of membrane proteins has been supported by the publication of 3D structures of almost 100 unique IMPs including two seven-helix transmembrane receptors [81]. Well-established expression systems for protein production, sophisticated isotope labeling schemes and cutting-edge NMR methods together with state-of-the-art spectrometers and innovative strategies to generate distance constraints are likely to provide more and larger membrane protein structures in the next few years. Furthermore, NMR spectroscopy can also provide dynamic and functional information at atomic resolution, providing unprecedented insights into the molecular mechanisms of ligand recognition, receptor activation and membrane–lipid interactions. Beyond the retinal protein field, 7-TM proteins and larger IMPs should benefit from the combination of the strategies established for PR and NpSRII, especially the most prominent members of the 7-TM class — the G-protein coupled receptors (GPCRs). These receptors play numerous critical roles in eukaryotic cells, but up to now, only a single structure — that of CXCR1 — has been obtained by combining a modeling approach with solid-state NMR-derived dipolar couplings [141]. More high-resolution NMR structures would allow detailed characterization of the dynamic and structural changes that occur upon receptor-binding with different ligands (agonists, reverse agonists and antagonists). A deeper understanding of these conformational changes will provide insights into mechanisms of ligand selectivity, biased signaling and GPCR activation, and facilitate the rational design of drugs aimed at these important pharmaceutical targets.

Acknowledgements

This work was supported by the EMBO fellowship ALTF 246-2011 and the Marie Curie FP7-PEOPLE-2011-IEF fellowship (grant 300330). I thank J.P. Kirkpatrick and S. Reckel for critical reading of the manuscript and L. Bailey for valuable and insightful discussions.

References

[1] J.P. Overington, B. Al-Lazikani, A.L. Hopkins, Opinion — how many drug targets are there? Nat. Rev. Drug Discov. 5 (2006) 993–996.
[2] H.M. Berman, J. Westbrook, Z. Feng, G. Gilliland, T.N. Bhat, H. Weissig, I.N. Shindyalov, P.E. Bourne, The Protein Data Bank, Nucleic Acids Res. 28 (2000) 235–242.
[3] R.M. Bill, P.J.F. Henderson, S. Iwata, E.R.S. Kunji, H. Michel, R. Neutze, S. Newstead, B. Poolman, C.G. Tate, H. Vogel, Overcoming barriers to membrane protein structure determination, Nat. Biotechnol. 29 (2011) 335–340.
[4] T. Qureshi, N.K. Goto, Contemporary methods in structure determination of membrane proteins by solution NMR, Top. Curr. Chem. 326 (2012) 123–185.
[5] S.G. Patching, NMR structures of polytopic integral membrane proteins, Mol. Membr. Biol. 28 (2011) 370–397.
[6] M. Hong, Y. Zhang, F. Hu, Membrane protein structure and dynamics from NMR spectroscopy, Annu. Rev. Phys. Chem. 63 (63) (2012) 1–24.
[7] P.J. Judge, A. Watts, Recent contributions from solid-state NMR to the understanding of membrane protein structure and function, Curr. Opin. Chem. Biol. 15 (2011) 690–695.
[8] K.H. Gardner, L.E. Kay, The use of ^{2}H, ^{13}C, ^{15}N multidimensional NMR to study the structure and dynamics of proteins, Annu. Rev. Biophys. Biomol. Struct. 27 (1998) 357–406.
[9] V. Tugarinov, V. Kanelis, L.E. Kay, Isotope labeling strategies for the study of high-molecular-weight proteins by solution NMR spectroscopy, Nat. Protoc. 1 (2006) 749–754.
[10] M. Zoonens, B. Miroux, Expression of membrane proteins at the *Escherichia coli* membrane for structural studies, Heterologous Expression of Membrane Proteins: Methods and Protocols, 601, 2010. 49–66.
[11] R.C. Page, J.D. Moore, H.B. Nguyen, M. Sharma, R. Chase, F.P. Gao, C.K. Mobley, C.R. Sanders, L. Ma, F.D. Sonnichsen, S. Lee, S.C. Howell, S.J. Opella, T.A. Cross, Comprehensive evaluation of solution nuclear magnetic resonance spectroscopy sample preparation for helical integral membrane proteins, J. Struct. Func. Genom. 7 (2006) 51–64.

[12] B. Miroux, J.E. Walker, Over-production of proteins in *Escherichia coli*: mutant hosts that allow synthesis of some membrane proteins and globular proteins at high levels, J. Mol. Biol. 260 (1996) 289–298.
[13] S. Wagner, M.M. Klepsch, S. Schlegel, A. Appel, R. Draheim, M. Tarry, M. Hogbom, K.J. van Wijk, D.J. Slotboom, J.O. Persson, J.-W. de Gier, Tuning *Escherichia coli* for membrane protein overexpression, Proc. Natl. Acad. Sci. U. S. A. 105 (2008) 14371–14376.
[14] B. Mouillac, J.-L. Baneres, Mammalian membrane receptors expression as inclusion bodies in *Escherichia coli*, Heterologous Expression of Membrane Proteins: Methods and Protocols, 601, 2010. 39–48.
[15] S. Hiller, R.G. Garces, T.J. Malia, V.Y. Orekhov, M. Colombini, G. Wagner, Solution structure of the integral human membrane protein VDAC-1 in detergent micelles, Science 321 (2008) 1206–1210.
[16] C. Fernandez, C. Hilty, G. Wider, P. Guntert, K. Wuthrich, NMR structure of the integral membrane protein OmpX, J. Mol. Biol. 336 (2004) 1211–1221.
[17] P.M. Hwang, W.Y. Choy, E.I. Lo, L. Chen, J.D. Forman-Kay, C.R.H. Raetz, G.G. Prive, R.E. Bishop, L.E. Kay, Solution structure and dynamics of the outer membrane enzyme PagP by NMR, Proc. Natl. Acad. Sci. U. S. A. 99 (2002) 13560–13565.
[18] A. Arora, F. Abildgaard, J.H. Bushweller, L.K. Tamm, Structure of outer membrane protein A transmembrane domain by NMR spectroscopy, Nat. Struct. Biol. 8 (2001) 334–338.
[19] J.R. Schnell, J.J. Chou, Structure and mechanism of the M2 proton channel of influenza A virus, Nature 451 (2008) 591-U512.
[20] K. Oxenoid, J.J. Chou, The structure of phospholamban pentamer reveals a channel-like architecture in membranes, Proc. Natl. Acad. Sci. U. S. A. 102 (2005) 10870–10875.
[21] W.D. Van Horn, H.-J. Kim, C.D. Ellis, A. Hadziselimovic, E.S. Sulistijo, M.D. Karra, C. Tian, F.D. Soennichsen, C.R. Sanders, Solution nuclear magnetic resonance structure of membrane-integral diacylglycerol kinase, Science 324 (2009) 1726–1729.
[22] S.H. Park, F. Casagrande, M. Chu, K. Maier, H. Kiefer, S.J. Opella, Optimization of purification and refolding of the human chemokine receptor CXCR1 improves the stability of proteoliposomes for structure determination, Biochim. Biophys. Acta Biomembr. 1818 (2012) 584–591.
[23] L. Arcemisbehere, T. Sen, L. Boudier, M.-N. Balestre, G. Gaibelet, E. Detouillon, H. Orcel, C. Mendre, R. Rahmeh, S. Granier, C. Vives, F. Fieschi, M. Damian, T. Durroux, J.-L. Baneres, B. Mouillac, Leukotriene BLT2 receptor monomers activate the G_{i2} GTP-binding protein more efficiently than dimers, J. Biol. Chem. 285 (2010) 6337–6347.
[24] Y. Zhou, T. Cierpicki, R.H.F. Jimenez, S.M. Lukasik, J.F. Ellena, D.S. Cafiso, H. Kadokura, J. Beckwith, J.H. Bushweller, NMR solution structure of the integral membrane enzyme DsbB: functional insights into DsbB-catalyzed disulfide bond formation, Mol. Cell 31 (2008) 896–908.
[25] M.J. Berardi, W.M. Shih, S.C. Harrison, J.J. Chou, Mitochondrial uncoupling protein 2 structure determined by NMR molecular fragment searching, Nature 476 (2011) 109-+.
[26] A. Gautier, H.R. Mott, M.J. Bostock, J.P. Kirkpatrick, D. Nietlispach, Structure determination of the seven-helix transmembrane receptor sensory rhodopsin II by solution NMR spectroscopy, Nat. Struct. Mol. Biol. 17 (2010) 768-U147.
[27] J. Tucker, R. Grisshammer, Purification of a rat neurotensin receptor expressed in *Escherichia coli*, Biochem. J. 317 (1996) 891–899.
[28] H.M. Weiss, R. Grisshammer, Purification and characterization of the human adenosine A_{2a} receptor functionally expressed in *Escherichia coli*, Eur. J. Biochem. 269 (2002) 82–92.
[29] Fc Neidhard, P.L. Bloch, D.F. Smith, Culture medium for enterobacteria, J. Bacteriol. 119 (1974) 736–747.
[30] J.I. Rhee, J. Bode, J.C. DiazRicci, D. Poock, B. Weigel, G. Kretzmer, K. Schugerl, Influence of the medium composition and plasmid combination on the growth of recombinant *Escherichia coli* JM109 and on the production of the fusion protein EcoRI::SPA, J. Biotechnol. 55 (1997) 69–83.
[31] O. Paliy, T.S. Gunasekera, Growth of *E. coli* BL21 in minimal media with different gluconeogenic carbon sources and salt contents, Appl. Microbiol. Biotechnol. 73 (2007) 1169–1172.
[32] M. Sattler, S.W. Fesik, Use of deuterium labeling in NMR: overcoming a sizeable problem, Structure 4 (1996) 1245–1249.
[33] O. Paliy, D. Bloor, D. Brockwell, P. Gilbert, J. Barber, Improved methods of cultivation and production of deuteriated proteins from *E. coli* strains grown on fully deuteriated minimal medium, J. Appl. Microbiol. 94 (2003) 580–586.
[34] R.L. Isaacson, P.J. Simpson, M. Liu, E. Cota, X. Zhang, P. Freemont, S. Matthews, A new labeling method for methyl transverse relaxation-optimized spectroscopy NMR spectra of alanine residues, J. Am. Chem. Soc. 129 (2007) 15428-+.
[35] Z. Serber, W. Straub, L. Corsini, A.M. Nomura, N. Shimba, C.S. Craik, P.O. de Montellano, V. Dotsch, Methyl groups as probes for proteins and complexes in in-cell NMR experiments, J. Am. Chem. Soc. 126 (2004) 7119–7125.
[36] S. Rajesh, D. Nietlispach, H. Nakayama, K. Takio, E.D. Laue, T. Shibata, Y. Ito, A novel method for the biosynthesis of deuterated proteins with selective protonation at the aromatic rings of Phe, Tyr and Trp, J. Biomol. NMR 27 (2003) 81–86.
[37] K.H. Gardner, M.K. Rosen, L.E. Kay, Global folds of highly deuterated, methyl-protonated proteins by multidimensional NMR, Biochemistry 36 (1997) 1389–1401.
[38] N.K. Goto, K.H. Gardner, G.A. Mueller, R.C. Willis, L.E. Kay, A robust and cost-effective method for the production of Val, Leu, Ile (δ1) methyl-protonated ^{15}N-, ^{13}C-, ^{2}H-labeled proteins, J. Biomol. NMR 13 (1999) 369–374.
[39] V.M. Bolanos-Garcia, O.R. Davies, Structural analysis and classification of native proteins from *E. coli* commonly co-purified by immobilised metal affinity chromatography, Biochim. Biophys. Acta Gen. Subj. 1760 (2006) 1304–1313.
[40] J.M. Cregg, J.L. Cereghino, J.Y. Shi, D.R. Higgins, Recombinant protein expression in *Pichia pastoris*, Mol. Biotechnol. 16 (2000) 23–52.
[41] H.A. van den Burg, P. de Wit, J. Vervoort, Efficient ^{13}C/^{15}N double labeling of the avirulence protein AVR4 in a methanol-utilizing strain (Mut^{+}) of *Pichia pastoris*, J. Biomol. NMR 20 (2001) 251–261.
[42] E. Rodriguez, N.R. Krishna, An economical method for ^{15}N/^{13}C isotopic labeling of proteins expressed in *Pichia pastoris*, J. Biochem. 130 (2001) 19–22.
[43] M. Tomida, M. Kimura, K. Kuwata, T. Hayashi, Y. Okano, S. Era, Development of a high-level expression system for deuterium-labeled human serum albumin, Jpn. J. Physiol. 53 (2003) 65–69.
[44] W.D. Morgan, A. Kragt, J. Feeney, Expression of deuterium-isotope-labelled protein in the yeast *Pichia pastoris* for NMR studies, J. Biomol. NMR 17 (2000) 337–347.
[45] S. Massou, V. Puech, F. Talmont, P. Demange, N.D. Lindley, M. Tropis, A. Milon, Heterologous expression of a deuterated membrane-integrated receptor and partial deuteration in methylotrophic yeasts, J. Biomol. NMR 14 (1999) 231–239.
[46] K. Egawa, H. Shibata, S.-i Yamashita, H. Yurimoto, Y. Sakai, H. Kato, Overexpression and purification of rat peroxisomal membrane protein 22, PMP22, in *Pichia pastoris*, Protein Expr. Purif. 64 (2009) 47–54.
[47] M. Shiroishi, T. Kobayashi, S. Ogasawara, H. Tsujimoto, C. Ikeda-Suno, S. Iwata, T. Shimamura, Production of the stable human histamine H_1 receptor in *Pichia pastoris* for structural determination, Methods 55 (2011) 281–286.
[48] Y. Fan, L. Shi, V. Ladizhansky, L.S. Brown, Uniform isotope labeling of a eukaryotic seven-transmembrane helical protein in yeast enables high-resolution solid-state NMR studies in the lipid environment, J. Biomol. NMR 49 (2011) 151–161.
[49] S. Emami, Y. Fan, R. Munro, V. Ladizhansky, L.S. Brown, Yeast-expressed human membrane protein aquaporin-1 yields excellent resolution of solid-state MAS NMR spectra, J. Biomol. NMR 55 (2013) 147–155.
[50] M.J. Wood, E.A. Komives, Production of large quantities of isotopically labeled protein in *Pichia pastoris* by fermentation, J. Biomol. NMR 13 (1999) 149–159.
[51] A.R. Pickford, J.M. O'Leary, Isotopic labeling of recombinant proteins from the methylotrophic yeast *Pichia pastoris*, Methods Mol. Biol. 278 (2004) 17–33.
[52] M.M. Whittaker, J.W. Whittaker, Construction and characterization of *Pichia pastoris* strains for labeling aromatic amino acids in recombinant proteins, Protein Expr. Purif. 41 (2005) 266–274.
[53] F. Junge, B. Schneider, S. Reckel, D. Schwarz, V. Doetsch, F. Bernhard, Large-scale production of functional membrane proteins, Cell Mol. Life Sci. 65 (2008) 1729–1755.
[54] C. Klammt, D. Schwarz, F. Loehr, B. Schneider, V. Doetsch, F. Bernhard, Cell-free expression as an emerging technique for the large scale production of integral membrane protein, FEBS J. 273 (2006) 4141–4153.
[55] D. Schwarz, F. Junge, F. Durst, N. Froelich, B. Schneider, S. Reckel, S. Sobhanifar, V. Doetsch, F. Bernhard, Preparative scale expression of membrane proteins in *Escherichia coli*-based continuous exchange cell-free systems, Nat. Protoc. 2 (2007) 2945–2957.
[56] C. Klammt, M.H. Perrin, I. Maslennikov, L. Renault, M. Krupa, W. Kwiatkowski, H. Stahlberg, W. Vale, S. Choe, Polymer-based cell-free expression of ligand-binding family B G-protein coupled receptors without detergents, Protein Sci. 20 (2011) 1030–1041.
[57] S. May, M. Andreasson-Ochsner, Z. Fu, Y.X. Low, D. Tan, H.-P.M. de Hoog, S. Ritz, M. Nallani, E.-K. Sinner, In vitro expressed GPCR inserted in polymersome membranes for ligand-binding studies, Angew. Chem. Int. Ed. 52 (2013) 749–753.
[58] S. Sobhanifar, S. Reckel, F. Junge, D. Schwarz, L. Kai, M. Karbyshev, F. Loehr, F. Bernhard, V. Doetsch, Cell-free expression and stable isotope labelling strategies for membrane proteins, J. Biomol. NMR 46 (2010) 33–43.
[59] S. Reckel, D. Gottstein, J. Stehle, F. Loehr, M.-K. Verhoefen, M. Takeda, R. Silvers, M. Kainosho, C. Glaubitz, J. Wachtveitl, F. Bernhard, H. Schwalbe, P. Guentert, V. Doetsch, Solution NMR structure of proteorhodopsin, Angew. Chem. Int. Ed. 50 (2011) 11942–11946.
[60] M. Etzkorn, T. Raschle, F. Hagn, V. Gelev, A.J. Rice, T. Walz, G. Wagner, Cell-free expressed bacteriorhodopsin in different soluble membrane mimetics: biophysical properties and NMR accessibility, Structure 21 (2013) 394–401.
[61] O. Soubias, K. Gawrisch, Rhodopsin–lipid interactions studied by NMR, Methods Enzymol. 522 (2013) 209–227.
[62] T. Zhuang, Q. Chen, M.-K. Cho, S.A. Vishnivetskiy, T.M. Iverson, V.V. Gurevich, C.R. Sanders, Involvement of distinct arrestin-1 elements in binding to different functional forms of rhodopsin, Proc. Natl. Acad. Sci. U. S. A. 110 (2013) 942–947.
[63] J.J. Liu, R. Horst, V. Katritch, R.C. Stevens, K. Wuethrich, Biased signaling pathways in β_2-adrenergic receptor characterized by ^{19}F-NMR, Science 335 (2012) 1106–1110.
[64] A.D. Gossert, A. Hinniger, S. Gutmann, W. Jahnke, A. Strauss, C. Fernandez, A simple protocol for amino acid type selective isotope labeling in insect cells with improved yields and high reproducibility, J. Biomol. NMR 51 (2011) 449–456.
[65] A. Strauss, F. Bitsch, B. Cutting, G. Fendrich, P. Graff, J. Liebetanz, M. Zurini, W. Jahnke, Amino-acid-type selective isotope labeling of proteins expressed in Baculovirus-infected insect cells useful for NMR studies, J. Biomol. NMR 26 (2003) 367–372.
[66] A. Strauss, F. Bitsch, G. Fendrich, P. Graff, R. Knecht, B. Meyhack, W. Jahnke, Efficient uniform isotope labeling of Abl kinase expressed in Baculovirus-infected insect cells, J. Biomol. NMR 31 (2005) 343–349.
[67] W.J. Walton, A.J. Kasprzakb, J.T. Hare, T.M. Logan, An economic approach to isotopic enrichment of glycoproteins expressed from Sf9 insect cells, J. Biomol. NMR 36 (2006) 225–233.
[68] M. Bruggert, T. Rehm, S. Shanker, J. Georgescu, T.A. Holak, A novel medium for expression of proteins selectively labeled with ^{15}N-amino acids in *Spodoptera frugiperda* (Sf9) insect cells, J. Biomol. NMR 25 (2003) 335–348.
[69] A.F.L. Creemers, C.H.W. Klaassen, P.H.M. Bovee-Geurts, R. Kelle, U. Kragl, J. Raap, W.J. de Grip, J. Lugtenburg, H.J.M. de Groot, Solid state ^{15}N NMR evidence for a

complex Schiff base counterion in the visual G-protein-coupled receptor rhodopsin, Biochemistry 38 (1999) 7195–7199.
[70] F. DeLange, C.H.W. Klaassen, S.E. Wallace-Williams, P.H.M. Bovee-Geurts, X.M. Liu, W.J. DeGrip, K.J. Rothschild, Tyrosine structural changes detected during the photoactivation of rhodopsin, J. Biol. Chem. 273 (1998) 23735–23739.
[71] M.C. Loewen, J. Klein-Seetharaman, E.V. Getmanova, P.J. Reeves, H. Schwalbe, H.G. Khorana, Solution ^{19}F nuclear Overhauser effects in structural studies of the cytoplasmic domain of mammalian rhodopsin, Proc. Natl. Acad. Sci. U. S. A. 98 (2001) 4888–4892.
[72] J. Klein-Seetharaman, P.J. Reeves, M.C. Loewen, E.V. Getmanova, L. Chung, H. Schwalbe, P.E. Wright, H.G. Khorana, Solution NMR spectroscopy of alpha-^{15}N lysine-labeled rhodopsin: the single peak observed in both conventional and TROSY-type HSQC spectra is ascribed to Lys-339 in the carboxyl-terminal peptide sequence, Proc. Natl. Acad. Sci. U. S. A. 99 (2002) 3452–3457.
[73] M. Eilers, P.J. Reeves, W.W. Ying, H.G. Khorana, S.O. Smith, Magic angle spinning NMR of the protonated retinylidene Schiff base nitrogen in rhodopsin: expression of ^{15}N-lysine- and ^{13}C-glycine-labeled opsin in a stable cell line, Proc. Natl. Acad. Sci. U. S. A. 96 (1999) 487–492.
[74] K. Werner, I. Lehner, H.K. Dhiman, C. Richter, C. Glaubitz, H. Schwalbe, J. Klein-Seetharaman, H.G. Khorana, Combined solid state and solution NMR studies of alpha, epsilon-^{15}N labeled bovine rhodopsin, J. Biomol. NMR 37 (2007) 303–312.
[75] K. Werner, C. Richter, J. Klein-Seetharaman, H. Schwalbe, Isotope labeling of mammalian GPCRs in HEK293 cells and characterization of the C-terminus of bovine rhodopsin by high resolution liquid NMR spectroscopy, J. Biomol. NMR 40 (2008) 49–53.
[76] V. Tugarinov, R. Muhandiram, A. Ayed, L.E. Kay, Four-dimensional NMR spectroscopy of a 723-residue protein: chemical shift assignments and secondary structure of malate synthase G, J. Am. Chem. Soc. 124 (2002) 10025–10035.
[77] K. Pervushin, R. Riek, G. Wider, K. Wuthrich, Transverse relaxation-optimized spectroscopy (TROSY) for NMR studies of aromatic spin systems in ^{13}C-labeled proteins, J. Am. Chem. Soc. 120 (1998) 6394–6400.
[78] Q. Zhang, R. Horst, M. Geralt, X. Ma, W.-X. Hong, M.G. Finn, R.C. Stevens, K. Wuethrich, Microscale NMR screening of new detergents for membrane protein structural biology, J. Am. Chem. Soc. 130 (2008) 7357–7363.
[79] D. Nietlispach, A. Gautier, Solution NMR studies of polytopic alpha-helical membrane proteins, Curr. Opin. Struct. Biol. 21 (2011) 497–508.
[80] A. Gautier, D. Nietlispach, Solution NMR studies of integral polytopic alpha-helical membrane proteins: the structure determination of the seven-helix transmembrane receptor sensory rhodopsin II, pSRII, Methods Mol. Biol. 914 (2012) 25–45.
[81] http://www.drorlist.com/nmr/MPNMR.html.
[82] C.L. Tian, M.D. Karra, C.D. Ellis, J. Jacob, K. Oxenoid, F. Sonnichsen, C.R. Sanders, Membrane protein preparation for TROSY NMR screening, Nucl. Magn. Reson. Biol. Macromol. C 394 (2005) 321–334.
[83] S. Hiller, G. Wagner, The role of solution NMR in the structure determinations of VDAC-1 and other membrane proteins, Curr. Opin. Struct. Biol. 19 (2009) 396–401.
[84] I. Maslennikov, C. Klammt, E. Hwang, G. Kefala, M. Okamura, L. Esquivies, K. Moers, C. Glaubitz, W. Kwiatkowski, Y.H. Jeon, S. Choe, Membrane domain structures of three classes of histidine kinase receptors by cell-free expression and rapid NMR analysis, Proc. Natl. Acad. Sci. U. S. A. 107 (2010) 10902–10907.
[85] C. Klammt, I. Maslennikov, M. Bayrhuber, C. Eichmann, N. Vajpai, E.J.C. Chiu, K.Y. Blain, L. Esquivies, J.H.J. Kwon, B. Balana, U. Pieper, A. Sali, P.A. Slesinger, W. Kwiatkowski, R. Riek, S. Choe, Facile backbone structure determination of human membrane proteins by NMR spectroscopy, Nat. Methods 9 (2012) 834-+.
[86] T.H. Bayburt, S.G. Sligar, Membrane protein assembly into nanodiscs, FEBS Lett. 584 (2010) 1721–1727.
[87] S.H. Park, S. Berkamp, G.A. Cook, M.K. Chan, H. Viadiu, S.J. Opella, Nanodiscs versus macrodiscs for NMR of membrane proteins, Biochemistry 50 (2011) 8983–8985.
[88] J.M. Glueck, M. Wittlich, S. Feuerstein, S. Hoffmann, D. Willbold, B.W. Koenig, Integral membrane proteins in nanodiscs can be studied by solution NMR spectroscopy, J. Am. Chem. Soc. 13 (2009) 12060-+.
[89] S.C. Lee, B.C. Bennett, W.-X. Hong, Y. Fu, K.A. Baker, J. Marcoux, C.V. Robinson, A.B. Ward, J.R. Halpert, R.C. Stevens, C.D. Stout, M.J. Yeager, Q. Zhang, Steroid-based facial amphiphiles for stabilization and crystallization of membrane proteins, Proc. Natl. Acad. Sci. U. S. A. 110 (2013) E1203–E1211.
[90] Q. Zhang, X. Ma, A. Ward, W.-X. Hong, V.-P. Jaakola, R.C. Stevens, M.G. Finn, G. Chang, Designing facial amphiphiles for the stabilization of integral membrane proteins, Angew. Chem. Int. Ed. 46 (2007) 7023–7025.
[91] K.-H. Park, C. Berrier, F. Lebaupain, B. Pucci, J.-L. Popot, A. Ghazi, F. Zito, Fluorinated and hemifluorinated surfactants as alternatives to detergents for membrane protein cell-free synthesis, Biochem. J. 403 (2007) 183–187.
[92] J.L. Popot, T. Althoff, D. Bagnard, J.L. Baneres, P. Bazzacco, E. Billon-Denis, L.J. Catoire, P. Champeil, D. Charvolin, M.J. Cocco, G. Cremel, T. Dahmane, L.M. de la Maza, C. Ebel, F. Gabel, F. Giusti, Y. Gohon, E. Goormaghtigh, E. Guittet, J.H. Kleinschmidt, W. Kuehlbrandt, C. Le Bon, K.L. Martinez, M. Picard, B. Pucci, J.N. Sachs, C. Tribet, C. van Heijenoort, F. Wien, F. Zito, M. Zoonens, Amphipols from A to Z, Annu. Rev. Biophys. 40 (40) (2011) 379–408.
[93] P.S. Chae, S.G.F. Rasmussen, R.R. Rana, K. Gotfryd, R. Chandra, M.A. Goren, A.C. Kruse, S. Nurva, C.J. Loland, Y. Pierre, D. Drew, J.-L. Popot, D. Picot, B.G. Fox, L. Guan, U. Gether, B. Byrne, B. Kobilka, S.H. Gellman, Maltose-neopentyl glycol (MNG) amphiphiles for solubilization, stabilization and crystallization of membrane proteins, Nat. Methods 7 (2010) 1003-U1090.
[94] S. Koutsopoulos, L. Kaiser, H.M. Eriksson, S. Zhang, Designer peptide surfactants stabilize diverse functional membrane proteins, Chem. Soc. Rev. 41 (2012) 1721–1728.
[95] D.E. Warschawski, A.A. Arnold, M. Beaugrand, A. Gravel, E. Chartrand, I. Marcotte, Choosing membrane mimetics for NMR structural studies of transmembrane proteins, Biochim. Biophys. Acta Biomembr. 1808 (2011) 1957–1974.
[96] T. Raschle, S. Hiller, M. Etzkorn, G. Wagner, Nonmicellar systems for solution NMR spectroscopy of membrane proteins, Curr. Opin. Struct. Biol. 20 (2010) 471–479.
[97] K.A. Baker, C. Tzitzilonis, W. Kwiatkowski, S. Choe, R. Riek, Conformational dynamics of the KcsA potassium channel governs gating properties, Nat. Struct. Mol. Biol. 14 (2007) 1089–1095.
[98] A. Gautier, J.P. Kirkpatrick, D. Nietlispach, Solution-state NMR spectroscopy of a seven-helix transmembrane protein receptor: backbone assignment, secondary structure, and dynamics, Angew. Chem. Int. Ed. 47 (2008) 7297–7300.
[99] T. Diercks, V. Truffault, M. Coles, O. Millett, Diagonal-free 3D/4D HN, HN-TROSY-NOESY-TROSY, J. Am. Chem. Soc. 132 (2010) 2138-+.
[100] A. Krejcirikova, V. Tugarinov, 3D-TROSY-based backbone and ILV-methyl resonance assignments of a 319-residue homodimer from a single protein sample, J. Biomol. NMR 54 (2012) 135–143.
[101] G. Zhu, Y.L. Xia, K.H. Sze, X.Z. Yan, 2D and 3D TROSY-enhanced NOESY of ^{15}N labeled proteins, J. Biomol. NMR 14 (1999) 377–381.
[102] K. Pervushin, R. Riek, G. Wider, K. Wuthrich, Attenuated T-2 relaxation by mutual cancellation of dipole–dipole coupling and chemical shift anisotropy indicates an avenue to NMR structures of very large biological macromolecules in solution, Proc. Natl. Acad. Sci. U. S. A. 94 (1997) 12366–12371.
[103] C. Fernandez, G. Wider, TROSY in NMR studies of the structure and function of large biological macromolecules, Curr. Opin. Struct. Biol. 13 (2003) 570–580.
[104] J.C.J. Barna, E.D. Laue, M.R. Mayger, J. Skilling, S.J.P. Worrall, Exponential sampling, an alternative method for sampling in two-dimensional NMR experiments, J. Magn. Reson. 73 (1987) 69–77.
[105] D. Rovnyak, D.P. Frueh, M. Sastry, Z.Y.J. Sun, A.S. Stern, J.C. Hoch, G. Wagner, Accelerated acquisition of high resolution triple-resonance spectra using non-uniform sampling and maximum entropy reconstruction, J. Magn. Reson. 170 (2004) 15–21.
[106] D.J. Holland, M.J. Bostock, L.F. Gladden, D. Nietlispach, Fast multidimensional NMR spectroscopy using compressed sensing, Angew. Chem. Int. Ed. 50 (2011) 6548–6551.
[107] M.J. Bostock, D.J. Holland, D. Nietlispach, Compressed sensing reconstruction of undersampled 3D NOESY spectra: application to large membrane proteins, J. Biomol. NMR 54 (2012) 15–32.
[108] M.K. Rosen, K.H. Gardner, R.C. Willis, W.E. Parris, T. Pawson, L.E. Kay, Selective methyl group protonation of perdeuterated proteins, J. Mol. Biol. 263 (1996) 627–636.
[109] Y. Shen, O. Lange, F. Delaglio, P. Rossi, J.M. Aramini, G. Liu, A. Eletsky, Y. Wu, K.K. Singarapu, A. Lemak, A. Ignatchenko, C.H. Arrowsmith, T. Szyperski, G.T. Montelione, D. Baker, A. Bax, Consistent blind protein structure generation from NMR chemical shift data, Proc. Natl. Acad. Sci. U. S. A. 105 (2008) 4685–4690.
[110] P. Robustelli, K. Kohlhoff, A. Cavalli, M. Vendruscolo, Using NMR chemical shifts as structural restraints in molecular dynamics simulations of proteins, Structure 18 (2010) 923–933.
[111] G. Cornilescu, F. Delaglio, A. Bax, Protein backbone angle restraints from searching a database for chemical shift and sequence homology, J. Biomol. NMR 13 (1999) 289–302.
[112] Y. Shen, F. Delaglio, G. Cornilescu, A. Bax, TALOS plus: a hybrid method for predicting protein backbone torsion angles from NMR chemical shifts, J. Biomol. NMR 44 (2009) 213–223.
[113] M.-S. Cheung, M.L. Maguire, T.J. Stevens, R.W. Broadhurst, DANGLE: a Bayesian inferential method for predicting protein backbone dihedral angles and secondary structure, J. Magn. Reson. 202 (2010) 223–233.
[114] D.S. Wishart, B.D. Sykes, F.M. Richards, The chemical-shift index — a fast and simple method for the assignment of protein secondary structure through NMR-spectroscopy, Biochemistry 31 (1992) 1647–1651.
[115] T.L. Hwang, P.C.M. van Zijl, S. Mori, Accurate quantitation of water-amide proton exchange rates using the phase-modulated CLEAN chemical EXchange (CLEANEX-PM) approach with a Fast-HSQC (FHSQC) detection scheme, J. Biomol. NMR 11 (1998) 221–226.
[116] W.F. Vranken, W. Boucher, T.J. Stevens, R.H. Fogh, A. Pajon, P. Llinas, E.L. Ulrich, J.L. Markley, J. Ionides, E.D. Laue, The CCPN data model for NMR spectroscopy: development of a software pipeline, Protein Struct. Funct. Genet. 59 (2005) 687–696.
[117] A.T. Brunger, P.D. Adams, G.M. Clore, W.L. DeLano, P. Gros, R.W. Grosse-Kunstleve, J.S. Jiang, J. Kuszewski, M. Nilges, N.S. Pannu, R.J. Read, L.M. Rice, T. Simonson, G.L. Warren, Crystallography & NMR system: a new software suite for macromolecular structure determination, Acta Crystallogr. D: Biol. Crystallogr. 54 (1998) 905–921.
[118] J.P. Linge, S.I. O'Donoghue, M. Nilges, Automated assignment of ambiguous nuclear overhauser effects with ARIA, Nucl. Magn. Reson. Biol. Macromol. B 339 (2001) 71–90.
[119] J.P. Linge, M. Habeck, W. Rieping, M. Nilges, ARIA: automated NOE assignment and NMR structure calculation, Bioinformatics 19 (2003) 315–316.
[120] P. Guntert, Automated NMR structure calculation with CYANA, Methods Mol. Biol. 278 (2004) 353–378.
[121] C.D. Schwieters, J.J. Kuszewski, N. Tjandra, G.M. Clore, The Xplor-NIH NMR molecular structure determination package, J. Magn. Reson. 160 (2003) 65–73.
[122] P. Guntert, Structure calculation of biological macromolecules from NMR data, Q. Rev. Biophys. 31 (1998) 145–237.

[123] R.S. Lipsitz, N. Tjandra, Residual dipolar couplings in NMR structure analysis, Annu. Rev. Biophys. Biomol. Struct. 33 (2004) 387–413.
[124] M. Ottiger, F. Delaglio, A. Bax, Measurement of J and dipolar couplings from simplified two-dimensional NMR spectra, J. Magn. Reson. 131 (1998) 373–378.
[125] N.C. Fitzkee, A. Bax, Facile measurement of ^{1}H–^{15}N residual dipolar couplings in larger perdeuterated proteins, J. Biomol. NMR 48 (2010) 65–70.
[126] K. Chen, N. Tjandra, The use of residual dipolar coupling in studying proteins by NMR, Top. Curr. Chem. 326 (2012) 47–67.
[127] Y. Ishii, M.A. Markus, R. Tycko, Controlling residual dipolar couplings in high-resolution NMR of proteins by strain induced alignment in a gel, J. Biomol. NMR 21 (2001) 141–151.
[128] R. Tycko, F.J. Blanco, Y. Ishii, Alignment of biopolymers in strained gels: a new way to create detectable dipole–dipole couplings in high-resolution biomolecular NMR, J. Am. Chem. Soc. 122 (2000) 9340–9341.
[129] S. Meier, D. Haussinger, S. Grzesiek, Charged acrylamide copolymer gels as media for weak alignment, J. Biomol. NMR 24 (2002) 351–356.
[130] T. Cierpicki, J.H. Bushweller, Charged gels as orienting media for measurement of residual dipolar couplings in soluble and integral membrane proteins, J. Am. Chem. Soc. 126 (2004) 16259–16266.
[131] J.J. Chou, S. Gaemers, B. Howder, J.M. Louis, A. Bax, A simple apparatus for generating stretched polyacrylamide gels, yielding uniform alignment of proteins and detergent micelles, J. Biomol. NMR 21 (2001) 377–382.
[132] H. Chen, F. Ji, V. Olman, C.K. Mobley, Y. Liu, Y. Zhou, J.H. Bushweller, J.H. Prestegard, Y. Xu, Optimal mutation sites for PRE data collection and membrane protein structure prediction, Structure 19 (2011) 484–495.
[133] S. Sobhanifar, B. Schneider, F. Loehr, D. Gottstein, T. Ikeya, K. Mlynarczyk, W. Pulawski, U. Ghoshdastider, M. Kolinski, S. Filipek, P. Guentert, F. Bernhard, V. Doetsch, Structural investigation of the C-terminal catalytic fragment of presenilin 1, Proc. Natl. Acad. Sci. U. S. A. 107 (2010) 9644–9649.
[134] D. Gottstein, S. Reckel, V. Doetsch, P. Guentert, Requirements on paramagnetic relaxation enhancement data for membrane protein structure determination by NMR, Structure 20 (2012) 1019–1027.
[135] P.M. Keizers, M. Ubbink, Paramagnetic tagging for protein structure and dynamics analysis, Prog. Nucl. Magn. Reson. Spectrosc. 58 (2011) 88–96.
[136] G. Otting, Protein NMR using paramagnetic ions, Annu. Rev. Biophys. 39 (39) (2010) 387–405.
[137] R.A. Laskowski, M.W. Macarthur, D.S. Moss, J.M. Thornton, PROCHECK — a program to check the stereochemical quality of protein structures, J. Appl. Crystallogr. 26 (1993) 283–291.
[138] R.A. Laskowski, J.A.C. Rullmann, M.W. MacArthur, R. Kaptein, J.M. Thornton, AQUA and PROCHECK-NMR: programs for checking the quality of protein structures solved by NMR, J. Biomol. NMR 8 (1996) 477–486.
[139] H. Luecke, B. Schobert, J.K. Lanyi, E.N. Spudich, J.L. Spudich, Crystal structure of sensory rhodopsin II at 2.4 angstroms: insights into color tuning and transducer interaction, Science 293 (2001) 1499–1503.
[140] A. Royant, P. Nollert, K. Edman, R. Neutze, E.M. Landau, E. Pebay-Peyroula, J. Navarro, X-ray structure of sensory rhodopsin II at 2.1-angstrom resolution, Proc. Natl. Acad. Sci. U. S. A. 98 (2001) 10131–10136.
[141] S.H. Park, B.B. Das, F. Casagrande, Y. Tian, H.J. Nothnagel, M. Chu, H. Kiefer, K. Maier, A.A. De Angelis, F.M. Marassi, S.J. Opella, Structure of the chemokine receptor CXCR1 in phospholipid bilayers, Nature 491 (2012) 779-+.